ELSEVIER

Catalysis Today 68 (2001) 135–143

CATALYSIS TODAY

www.elsevier.com/locate/cattod

Structure characterization of the Co and Ni catalysts for carbon dioxide reforming of methane

Rong Gang Ding, Zi Feng Yan*

State Key Laboratory for Heavy Oil Processing, University of Petroleum, Dongying 257062, PR China

Abstract

The effects of active components, promoters and reforming reaction on structure variation of catalysts for carbon dioxide reforming with methane are extensively investigated. It is found that the active component and promoters disperse in different sites on the support. The impregnated metal species may be mainly located on the inner surface of the micropore of the support. The 8.5%Ni–2%MgO–3%CeO_2/Al_2O_3 catalyst achieves best metal dispersion among the tested catalysts. It is also interesting to note that the addition of the alkaline oxide promoter (MgO) prohibits the metal dispersion on the support, while the addition of rare-earth metal oxide CeO_2 effectively promotes the Ni metal dispersion on the surface of the support despite of unsatisfactory self-dispersion of CeO_2 promoter.

Keywords: Carbon dioxide reforming with methane; Adsorption; Nickel catalyst; Promoter; Structure

1. Introduction

Conversion of methane and carbon dioxide into useful products is an important area in the current catalytic research on hydrocarbon transformations. Carbon dioxide reforming with methane is not only very important for potential usefulness in industry and environment optimization [1–5,9], but also theoretically significant in understanding the nature of heterogeneous catalysis on hydrocarbon conversion. Heterogeneous catalysis occurs at active centers on a surface and it is recognized that a complete understanding of the catalytic process requires a detailed knowledge of the nature and function of active sites on the surface of the catalysts. The key to surveying the active centers of the metal catalysts is to evaluate and characterize the structure features and properties of the catalysts. The variation of the properties of catalysts can reflect the interaction among metal, support and promoter and the agglomeration features of the active sites on the metal catalysts. The possible processes accompanying the carbon dioxide reforming with methane may be also speculated according to the changes of physical properties of catalysts. Although the structure characterization of the catalysts for carbon dioxide reforming with methane have been conducted recently, [6–8,10] a systematic structure variation of the Ni, Co catalysts before and after reforming reaction still need to be studied. In this paper, physical and chemical adsorption, X-ray diffraction (XRD), scanning electron microscope (SEM) and energy distribution using X-ray microanalysis (EDX) techniques are used to characterize the properties and structure of catalysts. The characterized results are used to correlate with the reforming reactivity on metal catalysts and to emphasize the importance

* Corresponding author. Present address: Department of Chemical Engineering, The University of Queensland, Brisbane, Qld 4072, Australia. Fax: +86-546-8393879.
E-mail addresses: rgding@cheque.uq.edu.au (R.G. Ding), zfyancat@sunctr.hdpu.edu.cn (Z.F. Yan).

0920-5861/01/$ – see front matter
PII: S0920-5861(01)00274-7

of the special structure features in the reaction of this type.

2. Experimental

2.1. Catalyst preparation

Two series of 20–40 mesh γ-alumina and silica supported Ni and Co catalysts were prepared by the incipient wetness impregnation using $CoSO_4$ (Co-1), $Co(NO_3)_2$ (Co-2), and $Ni(NO_3)_2$ as the metal precursors, respectively. The solids were dried overnight in air at 393 K, then calcined at 773 K in air for 6 h for complete decomposition of the precursors. For the promoted catalysts, magnesium nitrate and cerous nitrate were added to the support by the same method. The nickel loading was set from 7.0 to 11.5%, while each promoter content was kept from 0 to 3% (wt.%). Before the reaction, the catalyst was reduced at 873 K in a stream of H_2 for at least 2 h. The gas used was ultra high purity, 99.995%.

2.2. Catalytic reaction

The reforming reaction was carried out in a continuous flow quartz-fixed-bed reactor (i.d., 6 mm) under atmospheric pressure, at 973 K, and with a ratio of CH_4/CO_2 1.05. 150 mg catalyst was loaded into the reactor and weight hourly space velocity (WHSV) was controlled at 12.5 h^{-1}. The catalyst was reduced again in situ at the reaction temperature in the H_2 flow for 2 h. The flow rates of the feed gases were controlled by mass flow meters (Matheson Mass Flow Controller Model 8240). The temperature of the catalyst bed was measured by a chromel–alumel thermocouple, and it was kept constant within ±1 K. The composition of reactants/products mixture was analyzed with an on-line SP-3420 gas chromatograph equipped with a TCD and a Porapak QS column. The catalysts were characterized after 4 h reaction.

2.3. Catalyst characterization

The porous properties such as surface area, average pore diameter, and pore volume were determined using an ASAP 2010 analyzer using N_2 adsorption at 77.5 K. Samples were degassed at 673 K until the pressure in the tube was below 10 μm Hg before analysis.

The total pore volume, V_t, is derived from the amount of adsorption at a relatively pressure close to unity ($P/P_0 = 0.995$), given that the pores were totally filled with the liquid adsorbate. The average pore size, D_p, is estimated from the pore volume using the equation $D_p = 4V_t/S_{BET}$ by assuming a cylindrical pore geometry. The mesopore distribution curve is obtained from the adsorption branch of the N_2 isotherm by BJH method. The micropore distribution is calculated from the gas adsorption using the Horvath–Kawazoe equation, with relative pressure (P/P_0) below 0.01.

The dispersion of nickel on the support was roughly estimated by static equilibrium chemisorption of H_2 at rather isothermal conditions of 308 ± 0.1 K. A constant volume high-vacuum apparatus, ASAP 2010C, is used for this purpose. The vacuum reached 5 μm Hg by using the molecular drag pump in the chemisorption analysis. The physisorbed gaseous impurities on the surfaces of the catalyst samples are cleaned away by ultra high pure N_2 (99.999%) at 973 K. Subsequently, the samples are reduced in ultra high pure 30 ml/min H_2 flow (99.999%) at 973 K for 2 h. Finally, ultra high pure N_2 is introduced again to purge the samples for 30 min.

The chemisorption isotherms were measured at equilibrium pressures between 100 and 300 mm Hg. The initial analysis measured chemisorption and physisorption amount. The repeat analysis measured only physisorption amount. The difference between the initial and repeat analysis was the chemisorption amount of the sample. Uptake of H_2 at monolayer coverage of the Ni particles was obtained by extrapolation of the linear portion of the adsorption isotherms to zero pressure, which is a standard procedure.

A BDX-3200 X-ray powder diffractometer was used to identify the main phases of metal catalysts. Anode Cu Kα (40 kV, 20 mA) was employed as the X-ray radiation source, covering 2θ between 20° and 80°. The XRD patterns were monitored and processed by a computer.

The microscopic appearance observation was conducted using scanning electron microscope (JEM 5410LV, JEOL Technologies) with the accelerating voltage of 25 kV. The surface elemental composition of the catalysts was determined by energy distribution

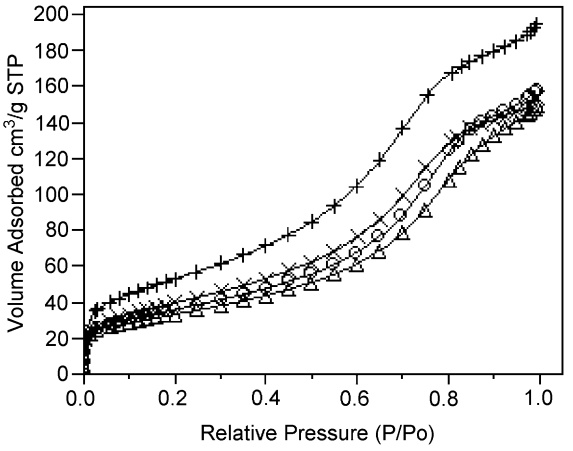

Fig. 1. The adsorption isotherm of the untreated support and calcined catalysts. (+) Untreated γ-Al_2O_3, (Δ) 10 wt.% Co-1/Al_2O_3 ($CoSO_4$ as the precursor), (×) 10 wt.% Co-2/Al_2O_3 ($Co(NO_3)_2$ as the precursor), (○) 10 wt.% Ni/Al_2O_3.

spectrum using X-ray microanalysis (ISIS, Oxford Instrument).

3. Results and discussion

3.1. Effect of active site on structure variation of catalysts

Fig. 1 showed the adsorption isotherms of the untreated alumina support and various calcined catalysts. All adsorption isotherms were similar to a type IV isotherm. Impregnation resulted in an approached decrease in the amount adsorbed, with only slight modification of the knee corresponding to adsorbate–adsorbent interaction.

Table 2
Effect of impregnation on the decrease in pore volume

Catalyst (wt.%)	V_{micro} (%)	V_{meso} (%)
10%Co-1/Al_2O_3	35.7	20.3
10%Co-2/Al_2O_3	31.1	18.5
10%Ni/Al_2O_3	35.7	15.0

A quantitative comparison of the variation of the textual structure, mesopore, and micropore distribution of the alumina support, fresh and used Co, Ni catalysts was given in Table 1. The results in Table 1 show that impregnation of sulfate or nitrate on the support decreases its surface area and total pore volume. However, the average pore diameters of all catalysts are increased after impregnation and carbon dioxide reforming reaction. Of interest is that the mean micropore diameters of all catalysts are obviously decreased after impregnating of the metal component on the alumina support. It means that the impregnated metal species maybe mainly locate on the inner surface of the micropore of the alumina support and that the reforming active sites locate in these micropore metal sites. Simultaneously, the larger pores are generated after reaction.

To evaluate the loss of pore volume by impregnation, the volume reductions in micropores and mesopores were calculated (Table 2). The calculation results indicate impregnation results in more blocking of the micropores. The pore size changes in Table 1 show that there is a peak shift toward smaller pore diameter for the catalysts in the range of micropore (with pore diameter <20 Å). The pore size is centered at 7.2 Å for the support, but they are centered at 5.9, 6.6 and 6.5 Å, respectively, for the catalysts. These

Table 1
The porous properties of the support and unpromoted catalysts[a]

Catalyst (10 wt.%)	State	S_{BET} (m^2/g)	D_p (Å)	D_{micro} (Å)	V_t (cm^3/g)	V_{micro} (cm^3/g)	V_{meso} (cm^3/g)
γ-Al_2O_3		192	62.5	7.20	0.300	0.054	0.246
Co-1/Al_2O_3	Fresh	118	78.0	5.90	0.231	0.035	0.196
	Used	114	85.7	6.31	0.244	0.030	0.214
Co-2/Al_2O_3	Fresh	144	66.0	6.60	0.238	0.038	0.200
	Used	174	97.1	6.67	0.422	0.040	0.383
Ni/Al_2O_3	Fresh	130	75.2	6.50	0.244	0.035	0.209
	Used	110	85.0	6.52	0.234	0.030	0.204

[a] D_p: average pore diameter. D_{micro}: mean micropore diameter.

Table 3
The porous properties of the support, promoted and unpromoted catalysts[a]

Catalyst (wt.%)	State	S_{BET} (m^2/g)	D_p (Å)	V_t (cm^3/g)	V_{micro} (cm^3/g)	V_{meso} (cm^3/g)
γ-Al_2O_3		192	62.5	0.300	0.054	0.246
7%Ni/Al_2O_3	Fresh	172	56.3	0.242	0.047	0.195
	Used	143	53.6	0.192	0.038	0.154
7%Ni–1%Mg–1%Ce/Al_2O_3	Fresh	180	55.3	0.240	0.045	0.195
8.5%Ni–2%Mg–3%Ce/Al_2O_3	Fresh	150	59.4	0.227	0.038	0.189
	Used	126	72.0	0.226	0.033	0.193
8.5%Ni–3%Mg–2%Ce/Al_2O_3	Fresh	148	57.0	0.212	0.039	0.173
8.5%Ni–3%Mg–3%Ce/Al_2O_3	Fresh	130	64.0	0.200	0.034	0.166
10%Ni–3%Mg–1%Ce/Al_2O_3	Fresh	144	63.3	0.227	0.036	0.191
	Used	123	69.0	0.212	0.032	0.181
11.5%Ni–1%Mg–2%Ce/Al_2O_3	Fresh	145	61.7	0.223	0.037	0.186
	Used	127	73.5	0.232	0.033	0.199
11.5%Ni–3%Ce/Al_2O_3	Fresh	143	71.5	0.255	0.036	0.219

[a] D_p: average pore diameter.

variations indicate that more pores are blocked in supermicropores (with pore diameter >7 Å) for catalysts and results in the reductions of micropore size and volume.

3.2. Effect of promoter on structure variation of catalysts

The variation of surface areas and total pore volumes of fresh and used catalysts with promoter addition were shown in Table 3. From the results shown in Table 1, it is deduced that nickel nitrate impregnate is possibly distributed uniformly in the surface pores of the support with similar decrease in micropore and mesopore volume for various catalysts. Compared the results in Table 3 with those in Table 1, it is easy to know that addition of oxide promoters results in the more decrease of the mesopore volume. Addition of promoters of $Mg(NO_3)_2$ and $Ce(NO_3)_2$ during the multiple-step impregnation process alters the deposition behaviors of $Ni(NO_3)_2$. The locations of the metal and oxide promoters are altered during the impregnation process and the oxide promoter are mostly concentrated on the outer layer of the alumina support while the nickel metal is generally dispersed in the support pores. Apparently, addition of promoters, which mostly deposit on the surface, contributes to more reduction in mesopore volume.

The unpromoted and promoted 7 wt.% Ni catalysts show very slight difference in micro- and mesopore volume, however, the variations are negligible and well within experimental errors. There is slight increase in surface area by the promoters' addition.

The pore structure variations of three kinds of 8.5 wt.% Ni catalysts in Table 3 show that more promoter addition results in more decrease in mesopore volume and the MgO addition exhibits stronger effect on this decrease. The data for 11.5 wt.% Ni catalysts also indicate that MgO addition significantly influences pore structure. Too much MgO addition may retard the reduction of NiO and cover the NiO layer on the support surface. Therefore, overloaded MgO may decrease the nickel dispersion and surface nickel concentration, which will be described in the H_2 chemisorption.

3.3. Effect of reaction on structure variation of catalysts

Fig. 2 showed that mesopore distribution of the untreated support, unpromoted and promoted catalysts before and after reaction. The variation of surface areas and total pore volumes of fresh and used catalysts were shown in Table 3.

Fig. 2 indicates that the number of pores in catalysts decreases after nickel is loaded on the support

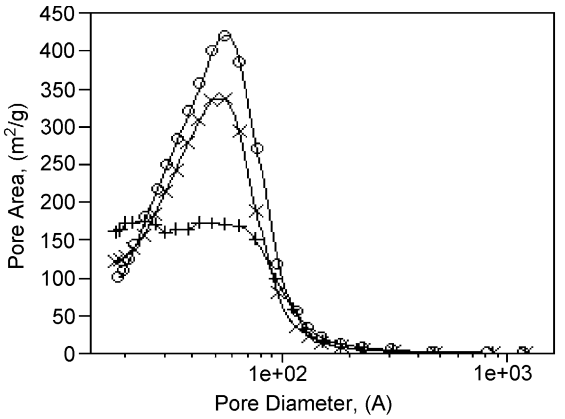

Fig. 2. The mesopore distribution of the untreated support, fresh and used Ni supported catalysts. (○) Untreated γ-Al_2O_3, (×) fresh 7 wt.%Ni/Al_2O_3, (+) used 7 wt.%Ni/Al_2O_3.

remaining in approximately same range of pore diameters. However, the pore size distribution of various catalysts is quite different after reaction. Fig. 2 shows that the volume of pores in the range of 30–80 Å in 7 wt.% Ni/Al_2O_3 catalyst is significantly decreased after reaction. The total pore volume is also decreased from 0.242 to 0.192 cm^3/g. The mesopore volume decrease contributes primarily to the decline of the total pore volume for 7 wt.% Ni/Al_2O_3 catalyst. The pore volume decrease may be derived from the coverage of carbon deposition produced in the reforming reaction. That is to say, carbon deposition mainly covers the surface of the catalyst and blocks the mesopores. The unpromoted catalyst exhibits poor resistivity to carbon deposition compared with the alkaline oxide-promoted catalysts according to the pore volume results before and after reaction.

The results shown in Table 3 indicate that the 8.5 wt.% Ni–2%MgO–3%CeO_2/Al_2O_3 provides almost unchanged total pore volume and decreased surface area after the reaction. The increased number of larger pores and decreased smaller pores generated in the reaction are responsible for these variations. The average pore diameter shifts toward larger pore size from 59.4 to 72.0 Å after reaction.

3.4. The metal dispersion variation of the nickel catalysts

The metal dispersions of the nickel catalysts supported on alumina were estimated by H_2 chemisorption with an assumption that each surface metal atom chemisorbs one hydrogen atom, i.e., $H/Ni_{surface} = 1$. Blank experiments show that the amount of H_2 chemisorbed on bare supports is negligibly small. The adsorption results were shown in Table 4.

It is found that the metal dispersions of Ni and metallic surface areas on all catalysts are not very high. The apparent low nickel dispersion on the high surface area of γ-Al_2O_3 carrier is probably due to the formation of $NiAl_2O_4$, which can not chemisorb hydrogen at room temperature. Incomplete reduction of Ni crystalline particles, as well as blocking and coverage of nickel crystallites by species originating from MgO and CeO_2 promoters, may also contribute to the small hydrogen adsorption amount.

Generally, larger surface area can be obtained by uniform dispersion [9]. Uniform dispersion of metal results in the fine metal particles. Appropriate particle size is necessary for the structure-facile catalysts. However, for most metal supported catalysts, the catalytic activity becomes higher with finer active metal particles. The catalytic performance of the supported metal catalysts significantly depends on the metal crystalline particle size and distribution. Simultaneously, metal dispersion on the support is strongly dependent on the distribution of the active phase within the support and on the type and degree of interaction reached [11].

Table 4
The metal dispersions and metallic surface areas of the catalysts

Catalyst (wt.%)	M_{disp} (%)	M_{sa} (m^2/g sample)	N_{sa} (m^2/g metal)
8.5%Ni–2%MgO–3%CeO_2/Al_2O_3	0.313	0.177	2.08
8.5%Ni–3%MgO–3%CeO_2/Al_2O_3	0.113	0.064	0.752
7%Ni–1%MgO–1%CeO_2/Al_2O_3	0.204	0.095	1.35
10%Ni–2%MgO/Al_2O_3	0.170	0.114	1.13

The results show that the 8.5% Ni–2%MgO–3 %CeO_2/Al_2O_3 catalyst achieves best metal dispersion among the tested catalysts. The nickel dispersion declines from 0.313 to 0.113% with increased MgO addition from 2 to 3 wt.%. This may be attributed partly to the catalyst preparation uncertainty. However, no doubt that the decrease of metal dispersion can be ascribed primarily to the overloaded promoter. Overloaded MgO may cover NiO dispersed on the surface of the catalysts and decrease the dispersion of NiO.

3.5. Crystalline phase changes of the catalysts

The XRD patterns of the support and the promoted and unpromoted nickel based catalysts were shown in Fig. 3. From the comparison of the XRD spectra of support and catalysts, it is clearly observed that NiO diffraction peak does not appear in the spectra of unpromoted and promoted nickel based catalysts. It is a good indication that high dispersion of nickel oxide is achieved over γ-Al_2O_3 support. However, it is difficult to estimate the effect of promoters on the metal dispersion on the support according to the XRD patterns.

As can be derived from the XRD spectra shown in Fig. 3, there exists no detectable solid reaction between NiO and Al_2O_3 over promoted catalyst. However, certain amounts of nickel are found in the form of $NiAl_2O_4$, a compound resulting from the solid reaction between NiO and the acidic Al_2O_3 support in the Ni/Al_2O_3 catalyst. The $NiAl_2O_4$ crystalline phase, which has a stable spinel structure, is rather difficult to be reduced, as witnessed by the fact that it essentially survives H_2 reduction at 1023 K [12]. However, addition of MgO (3 wt.%) to γ-Al_2O_3 significantly affects the basicity/acidity of the support, leading to a profound change in the bulk phase composition. It is observed that the diffraction peak of $NiAl_2O_4$ disappears over alkaline metal oxide promoted catalyst. This is probably attributed to the fact that the basic MgO is preferably reacting with the acidic Al_2O_3 to form stable magnesium aluminate, thereby suppressing the reaction between NiO and Al_2O_3.

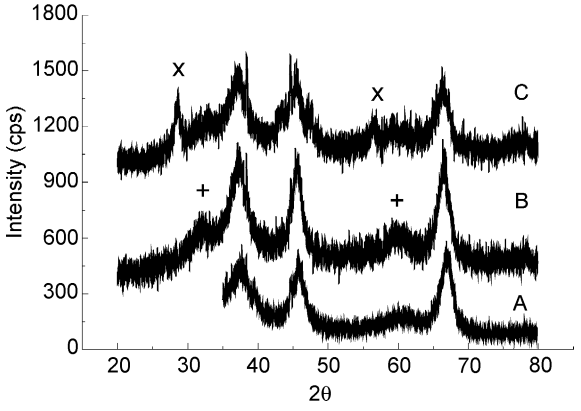

Fig. 3. The XRD patterns of Al_2O_3 support, unpromoted and promoted catalysts calcined at 873 K: ((+) $NiAl_2O_4$, (×) CeO_2); A: γ-Al_2O_3, B: 8.5 wt.%Ni/γ-Al_2O_3, C: 8.5 wt.%Ni–2 wt.%MgO–3 wt.%CeO_2/γ-Al_2O_3.

The emergence of CeO_2 diffraction peak in $Ni–Mg–Ce/Al_2O_3$ catalyst indicates that the dispersion of CeO_2 is not satisfied. This may be related to the catalyst preparation processes and conditions. More series tests of the influence of CeO_2 addition on the dispersion of metal are absent now. The well dispersion of CeO_2 added in an appropriate amount into Ni catalysts with or without other promoters is also an interesting topic worth further studying. The $Ni–Mg–Ce/Al_2O_3$ catalyst exhibits perfect performance in the catalyst evaluation experiments despite of unsatisfactory dispersion of CeO_2 promoter. The EDX analysis explains the emergence of the CeO_2 diffraction peak perfectly in following section. In contrast to CeO_2, the dispersion of MgO promoter is satisfactory and no diffraction peak appeared in the XRD patterns of the promoted catalyst.

3.6. The surface composition and morphology of the catalysts

The surface elemental compositions of the fresh and used catalysts were characterized by EDX analysis and the results were shown in Tables 5 and 6. Table 5 showed the relative content of selected elements and Table 6 showed the full element composition of surfaces of the catalysts.

The high surface concentration of some element indicates that uniform dispersion of the element is achieved. The enrichment trend of the element may be effectively retarded and various states of the element essentially exist in relatively small particles. From Table 5 it is observed that the surface concentration

Table 5
The surface composition of the selected element of the catalysts[a]

Catalyst (wt.%)	State	Al (%)	Ni (%)	Mg (%)	Ce (%)
7%Ni/Al_2O_3	Fresh	94.71	5.29	–	–
	Used	97.63	2.37	–	–
8.5%Ni–2%MgO–3%CeO_2/Al_2O_3	Fresh	84.31	9.18	n.d.	6.51
	Used	84.74	10.61	n.d.	4.65
10%Ni–2%MgO/Al_2O_3	Fresh	94.26	5.74	n.d.	–
	Used	95.80	4.21	n.d.	–
11.5%Ni–3%–CeO_2/Al_2O_3	Fresh	93.04	4.18	–	2.78

[a] n.d.: not detected. %: atomic percentage.

of the Ni over unpromoted catalyst significantly decreased from 5.29 to 2.37% after the reaction. The surface concentration of Ni element also declined to some extent from 5.74 to 4.21% over the MgO promoted catalyst after reaction. However, it is interesting that the surface concentrations of Ni element increases over CeO_2 promoted catalysts after reaction.

For the Ce-promoted catalysts, the nickel loadings on the support were higher than that of Ce-missing catalysts. High nickel loading does not favor the dispersion of Ni on the surface of the support. However, the surface concentration of Ni reaches 4.18% on the fresh 11.5%Ni–3%Ce/Al_2O_3 catalyst, approached that on the fresh 7.5%Ni/Al_2O_3 catalyst. The uniform dispersion of nickel component over the 8.5%Ni loaded catalyst may be ascribed to appropriate nickel loading. Lu et al. [13] studied the optimum nickel loading on various supports. The results showed that two-dimensional surface compound was formed by the interaction between NiO and Al_2O_3 with nickel loading set at 9.0% under the specific conditions. The two-dimensional surface compound was highly dispersed on the surface of the support, and thus resulted in the maximum dispersion of Ni metal particles. Too high nickel loading may result in the formation of NiO crystalline phase on the support. The NiO crystalline phase submits little contribution to nickel dispersion, and large Ni particles are prone to formation in the reduction process. The large Ni particles provide less active metal surface area and cause rapid deactivation by carbon deposition on the Ni particles.

The high surface concentration of Ni on the 8.5%Ni–2%MgO–3%CeO_2/Al_2O_3 may be derived from two causes. The appropriate nickel loading is the key to obtaining uniform dispersion on the surface of the Al_2O_3 support. As mentioned above, two-dimensional surface compound may be formed by the interaction between NiO and Al_2O_3 on the catalyst and Ni particles were highly dispersed under the specific conditions. Additionally, the comparison of the surface compositions of the catalysts gives good indication that the addition of rare-earth metal oxide CeO_2 effectively promotes the Ni metal dispersion on

Table 6
The surface composition of the full element of the catalysts[a]

Catalyst (wt.%)	State	Al (%)	Ni (%)	Mg (%)	Ce (%)	Si (%)	Na (%)	C (%)	O (%)
7%Ni–3%MgO–3%CeO_2/Al_2O_3	Fresh	–	6.95	1.65	0.35	18.4	–	–	72.7
	Used	–	3.38	0.22	0.11	4.36	–	80.3	11.6
8.5%Ni–3%MgO–3%CeO_2/Al_2O_3	Fresh	25.4	2.8	1.21	0.48	–	2.83	–	67.3
	Red.	27.7	2.96	1.29	0.83	–	2.26	–	65.0
	Used	15.6	2.06	0.67	0.32	–	1.72	21.5	58.1
8.5%Ni–2%MgO–3%CeO_2/Al_2O_3	Fresh	25.5	3.38	0.43	0.38	–	0.46	–	68.5

[a] %: atomic percentage, red: reduced.

the surface of the catalysts. Furthermore, the nickel component is gradually dispersed on the surface of the support following the exposure to reaction gas mixture for a period.

Chen et al. [14] investigated the influence of the rare-earth metal oxide on the nickel dispersion on the Al_2O_3 support. They reported that the active metal component did not directly stick to the support, but to the surface of the rare-earth metal oxide. The interaction between them occurred and the specific structure with filling was formed on the support. This structure inhibited the migration and enrichment of Ni and improved the nickel dispersion in the catalyst preparation and reaction processes. The formation of stable spinel $NiAl_2O_4$ was also retarded to a reasonable content.

It is also noteworthy that the change of the self-dispersion of CeO_2 on the support. The surface concentration of Ce decreased from 6.51 to 4.65% on the MgO-containing catalyst and increased from 2.78 to 5.19% on the MgO-deficient catalyst after reaction. The surface concentration of Ce decreased from 6.51 to 4.28% when the MgO addition increased from 2 to 3% for the fresh catalysts. Apparently, the addition of MgO inhibits the dispersion of CeO_2 on the catalysts. Therefore, the appearance of CeO_2 diffraction peak on the XRD patterns of 8.5%Ni–2%MgO–3%CeO_2/Al_2O_3 catalyst is indicative of the undesirable self-dispersion of CeO_2 promoter. The EDX analysis results are in good harmony with the XRD experiment results.

The comparison of the Ni–Mg–Ce/Al_2O_3 catalysts with different MgO contents exhibits that increased MgO addition inhibits the promotion effect of CeO_2 on Ni dispersion. Therefore, the optimum combination of the addition amount of the promoters is very important for perfect metal dispersion and desirable catalyst performance in the carbon dioxide reforming with methane.

The comparison of Figs. 4 and 5 shows that severe carbon deposition occurs on the Ni–Mg–Ce/SiO_2 catalyst after the reaction and the surface concentration of carbon reaches 80.3% (Table 6). The results indicate that the surface carbon is the dominant element on used Ni–Mg–Ce/SiO_2 catalyst. The carbon deposition results in the significant decrease of the surface concentrations of Ni, Mg and Ce. The sharp decline of surface concentration of Si and O are also clearly demonstrated. The variations of surface elemental

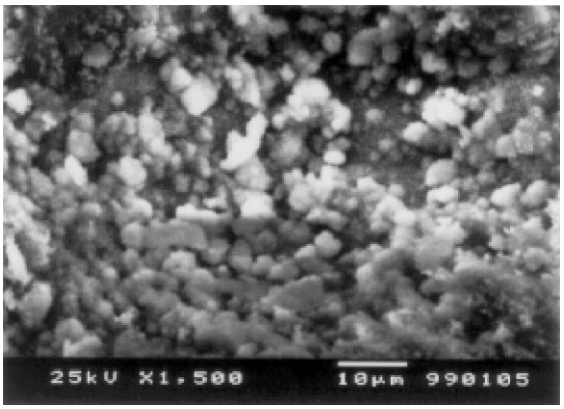

Fig. 4. The SEM photograph of fresh 7 wt.%Ni–3 wt.%MgO–3 wt.%CeO_2/SiO_2 catalyst.

concentration give good evidence that carbon deposits not only on the surfaces of metal active sites but also on the support.

It is observed that the surface of catalyst is covered with loose carbon structure and large nickel crystalline particles from the SEM photo of used Si-containing catalyst (Fig. 5). Nickel crystalline size of the used catalyst is increased indicating that sintering of catalyst occurs in the tested catalyst. Fig. 6 shows that the degree of sintering is not so appreciable for Ni–Mg–Ce/Al_2O_3.

It has been suggested that catalyst support influence the coke resistivity of nickel catalyst via stabilization of different CH_x surface intermediates. Osaki

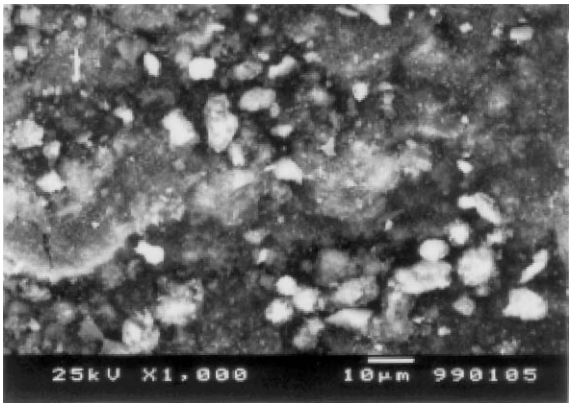

Fig. 5. The SEM photograph of used 7 wt.%Ni–3 wt.%MgO–3 wt.%CeO_2/SiO_2 catalyst.

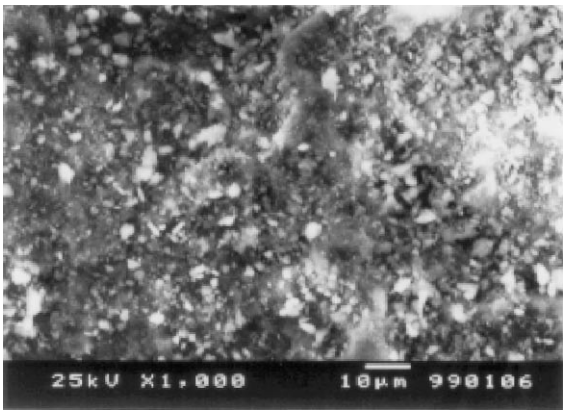

Fig. 6. The SEM photograph of used 8.5 wt.%Ni–3 wt.%MgO–3 wt.%CeO_2/Al_2O_3 catalyst.

et al. [15] used pulse surface reaction rate analysis to study CH_4/CO_2 reforming and found that the more hydrogen-deficient CH_x led to more carbon deposition. The values of the number of hydrogen in CH_x were as follows: $x = 2.7$ for Ni/MgO, 2.4 for Ni/Al_2O_3, 1.9 for Ni/TiO_2, and 1.0 for Ni/SiO_2. Accordingly, Ni/MgO is, therefore, more resistant to carbon deposition than Ni/Al_2O_3 and Ni/SiO_2. This probably explained the more carbon deposition on Ni/SiO_2 catalyst than on Ni/Al_2O_3 catalyst.

4. Conclusions

1. The mean micropore diameters of all catalysts were obviously decreased after impregnating of the metal component on the alumina support. It means that the impregnated metal species may be mainly locate on the inner surface of the micropore of the alumina support and that the reforming active sites also locate in these micropore metal sites.
2. The oxide promoter were mostly concentrated on the outer layer of the alumina support while the nickel metal was generally dispersed in the support pores. Addition of promoters contributed to more reduction in mesopore volume.
3. The addition of the alkaline oxide MgO promoter significantly prohibits the metal dispersion on the catalyst. Good dispersion of nickel oxide and MgO promoter is achieved over γ-Al_2O_3 support. Addition of MgO promoter effectively retards the formation of $NiAl_2O_4$ phase, however, overloaded MgO promoter can result in sharp decrease of the metal dispersion.
4. The addition of rare-earth metal oxide CeO_2 effectively promotes the Ni metal dispersion on the surface of the catalysts despite of undesirable self-dispersion of CeO_2 promoter. Furthermore, the nickel component is gradually dispersed on the surface of the support following the exposure to reaction gas mixture for a period. The addition of MgO inhibited the self-dispersion and promotion effect of CeO_2 on Ni dispersion on the catalysts.

Acknowledgements

Financial supports by the Young Scientists Award Foundation of Shandong Province and China National Petroleum Corporation are gratefully acknowledged.

References

[1] H.M. Swaan, V.C.H. Kroll, G.A. Martin, C. Mirodatos, Catal. Today 21 (1994) 571–578.
[2] Y.H. Hu, E. Ruckenstein, Catal. Lett. 43 (1997) 71–79.
[3] E. Ruckenstein, Y.H. Hu, Appl. Catal. 133 (1995) 149–161.
[4] Y.H. Hu, E. Ruckenstein, Catal. Lett. 36 (1996) 145–156.
[5] T. Horiuchi, K. Sakuma, T. Fukui, Y. Kubo, T. Osaki, T. Mori, Appl. Catal. 144 (1996) 111–120.
[6] Z. Zhang, X.E. Verykios, Appl. Catal. 138 (1996) 109–133.
[7] Z. Zhang, X.E. Verykios, Catal. Today 21 (1994) 589–595.
[8] V.A. Tsipouriari, A.M. Efstathiou, X.E. Verkios, Catal. Today 21 (1994) 579–587.
[9] C. Cheng, in: C. Cheng (Ed.), Physical Chemistry of Surface, Science and Technology, Literature Press, Beijing, 1995, pp. 304–308 (Chapter 4).
[10] P. Gronchi, P. Centola, R. Del Rosso, Appl. Catal. 68 (1989) 990–994.
[11] S.B. Wang, G.Q. Lu, Ind. Eng. Chem. Res. 36 (1997) 5103–5109.
[12] Z.L. Zhang, X.E. Verykios, S.M. MacDonald, J. Phys. Chem. 100 (1996) 744–754.
[13] Y. Lu, C.C. Yu, Chinease J. Catal. 17 (3) (1996) 212–217.
[14] Y.G. Chen, J. Ren, D. Wu, W.H. Fan, Petrochemical 23 (12) (1994) 771–775.
[15] T. Osaki, H. Masuda, T. Mori, Catal. Lett. 29 (1994) 33–37.